

Three-gluon contribution to the single spin asymmetry for light hadron production in pp collision

HIROO BEPPU¹, KOICHI KANAZAWA^{1,2}, YUJI KOIKE³ AND SHINSUKE YOSHIDA^{4,5}

¹ *Graduate School of Science and Technology, Niigata University, Ikarashi, Niigata
950-2181, Japan*

² *Department of Physics, Barton Hall, Temple University, Philadelphia, Pennsylvania
19122, USA*

³ *Department of Physics, Niigata University, Ikarashi, Niigata 950-2181, Japan*

⁴ *Theoretical Research Division, Nishina Center, RIKEN, Wako 351-0198, Japan*

⁵ *Physics Department, Brookhaven National Laboratory, Upton, NY 11973, USA*

Abstract

We study the twist-3 three-gluon contribution to the single spin asymmetry in the light-hadron production in pp collision in the framework of the collinear factorization. We derive the corresponding cross section formula in the leading order with respect to the QCD coupling constant. We also present a numerical calculation of the asymmetry at the RHIC energy, using a model for the three-gluon correlation functions suggested by the asymmetry observed in the D -meson production at RHIC.

1 Introduction

The large single spin asymmetry (SSA) $A_N \equiv (\sigma^\uparrow - \sigma^\downarrow)/(\sigma^\uparrow + \sigma^\downarrow)$ for the light-hadron productions, $p^\uparrow p \rightarrow hX$ ($h = \pi, K, \eta$), observed by the Relativistic Heavy Ion collider (RHIC) at the Brookhaven National Laboratory (BNL) [1]-[8] is the cleanest data which can be analyzed by means of the twist-3 mechanism in the framework of the collinear factorization. This process receives, in principle, four types of the twist-3 contributions depending on the type of the twist-3 correlation function participating in the cross section; i.e., (i) twist-3 quark-gluon correlation functions in the polarized nucleon [9]-[15], (ii) twist-3 three-gluon correlation functions in the polarized nucleon [16]-[21], (iii) twist-3 fragmentation function for the final hadron [22]-[25] and (iv) twist-3 quark-gluon correlation function in the initial unpolarized nucleon [26]. The last contribution (iv) was shown to be negligible due to the small partonic hard cross sections [27]. So far the data of A_N for the light-hadron production has been analyzed by assuming that the contribution (i) saturates the whole asymmetry [13, 28, 29, 30]. Although the gross feature of the observed asymmetry has been well reproduced by these analyses, the above (ii) and (iii) could also become an important sources of the asymmetry. Furthermore, the sign of the quark-gluon correlation functions in the above analysis is opposite to what is expected from the analysis of SSAs observed in semi-inclusive deep inelastic scattering (SIDIS) [31]. Therefore it is important to perform a global analysis of the SSAs for variety of processes including the whole contributions. The cross section formula for (iii) was derived only recently [25], while the formula for (ii) is not available in the literature.

In our recent papers, we have derived the contribution from the twist-3 three-gluon correlation functions to SSA for the D -meson productions in SIDIS, $ep^\uparrow \rightarrow eDX$ [18, 32], and the pp collision, $p^\uparrow p \rightarrow DX$ [20], and the Drell-Yan/direct-photon processes, $p^\uparrow p \rightarrow \gamma^{(*)}X$ [21]. Using some models for the three-gluon correlation functions, we also studied its impact on the corresponding asymmetries at the energy of RHIC and the Electron-Ion-Collider (EIC), and showed the sensitivity of the asymmetries to the form of the three-gluon correlation functions.

The purpose of this paper is to derive the three-gluon contribution to SSA for the light-hadron production in the pp collision by applying the formalism developed for the above processes. This will complete the corresponding leading order twist-3 cross section together with the known result for the above contributions (i) and (iii). Our presentation in this paper will be brief, referring the readers to [18, 19, 20, 21] for the detail of the calculation. After introducing the three-gluon correlation functions in section 2, we present the twist-3 cross section in section 3. In section 4, we study its impact on the SSA in the light-hadron productions at the RHIC energy by using the model in [20, 21]. We will see the three-gluon correlation disturbs the asymmetry reproduced by the quark-gluon correlation functions in [28, 29], which shows that this process may be used to constrain the magnitude and the form of the three-gluon correlations.

2 Three-gluon correlation functions in the transversely polarized nucleon

As clarified in [16, 17, 18], there are two independent three-gluon correlation functions in the transversely polarized nucleon, $O(x_1, x_2)$ and $N(x_1, x_2)$, which are the Lorentz-scalar functions of the longitudinal momentum fractions x_1 and x_2 , defined as

$$\begin{aligned} O^{\alpha\beta\gamma}(x_1, x_2) &= -g(i)^3 \int \frac{d\lambda}{2\pi} \int \frac{d\mu}{2\pi} e^{i\lambda x_1} e^{i\mu(x_2-x_1)} \langle pS_\perp | d_{bca} F_b^{\beta n}(0) F_c^{\gamma n}(\mu n) F_a^{\alpha n}(\lambda n) | pS_\perp \rangle \\ &= 2iM_N \left[O(x_1, x_2) g^{\alpha\beta} \epsilon^{\gamma pn S_\perp} + O(x_2, x_2 - x_1) g^{\beta\gamma} \epsilon^{\alpha pn S_\perp} + O(x_1, x_1 - x_2) g^{\gamma\alpha} \epsilon^{\beta pn S_\perp} \right], \end{aligned} \quad (1)$$

$$\begin{aligned} N^{\alpha\beta\gamma}(x_1, x_2) &= -g(i)^3 \int \frac{d\lambda}{2\pi} \int \frac{d\mu}{2\pi} e^{i\lambda x_1} e^{i\mu(x_2-x_1)} \langle pS_\perp | i f_{bca} F_b^{\beta n}(0) F_c^{\gamma n}(\mu n) F_a^{\alpha n}(\lambda n) | pS_\perp \rangle \\ &= 2iM_N \left[N(x_1, x_2) g^{\alpha\beta} \epsilon^{\gamma pn S_\perp} - N(x_2, x_2 - x_1) g^{\beta\gamma} \epsilon^{\alpha pn S_\perp} - N(x_1, x_1 - x_2) g^{\gamma\alpha} \epsilon^{\beta pn S_\perp} \right], \end{aligned} \quad (2)$$

where $F_a^{\alpha\beta} \equiv \partial^\alpha A_a^\beta - \partial^\beta A_a^\alpha + g f_{abc} A_b^\alpha A_c^\beta$ is the gluon's field strength, and we used the notation $F_a^{\alpha n} \equiv F_a^{\alpha\beta} n_\beta$ and $\epsilon^{\alpha pn S_\perp} \equiv \epsilon^{\alpha\mu\nu\lambda} p_\mu n_\nu S_{\perp\lambda}$ with the convention $\epsilon_{0123} = 1$. d^{bca} and f^{bca} are the symmetric and anti-symmetric structure constants of the color SU(3) group, and we have suppressed the gauge-link operators which ensure the gauge invariance. p is the nucleon momentum, and S_\perp is the transverse spin vector of the nucleon normalized as $S_\perp^2 = -1$. In the twist-3 accuracy, p can be regarded as lightlike ($p^2 = 0$), and n is another lightlike vector satisfying $p \cdot n = 1$. To be specific, we set $p^\mu = (p^+, 0, \mathbf{0}_\perp)$, $n^\mu = (0, n^-, \mathbf{0}_\perp)$, and $S_\perp^\mu = (0, 0, \mathbf{S}_\perp)$. The nucleon mass M_N is introduced to define $O(x_1, x_2)$ and $N(x_1, x_2)$ dimensionless. The decomposition (1) and (2) takes into account all the constraints from hermiticity, invariance under the parity- and time-reversal transformations and the permutation symmetry among the participating three gluon-fields. The functions $O(x_1, x_2)$ and $N(x_1, x_2)$ are real and have the following symmetry properties,

$$O(x_1, x_2) = O(x_2, x_1), \quad O(x_1, x_2) = O(-x_1, -x_2), \quad (3)$$

$$N(x_1, x_2) = N(x_2, x_1), \quad N(x_1, x_2) = -N(-x_1, -x_2). \quad (4)$$

The functions $N(x_1, x_2)$ and $O(x_1, x_2)$ are, respectively, even and odd under charge conjugation.

3 Twist-3 cross section for $p^\uparrow p \rightarrow hX$ induced by the three-gluon correlation functions

The twist-3 single-spin-dependent cross section for the process $p^\uparrow(p, S_\perp) + p(p') \rightarrow h(P_h) + X$ induced by the three-gluon correlation functions can be obtained by applying the formalism

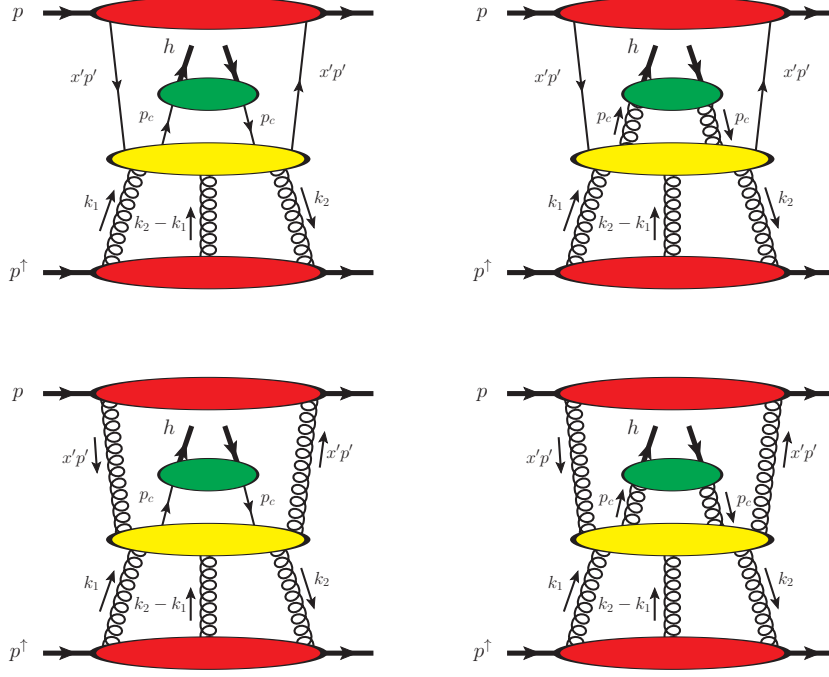


Figure 1: Schematic diagrams for the contribution of the three-gluon correlation functions to the SSA in the light-hadron production $p^\uparrow p \rightarrow hX$. The four blobs in each diagram represent, from the bottom to top, three-gluon correlation (6), the partonic hard part (5), the fragmentation function for the final hadron and the unpolarized parton distribution in the initial nucleon, respectively.

developed in [18, 19, 20, 21]. Figure 1 shows the cut diagrams for the cross section. There the partonic hard part (second bottom blob),

$$S_{\mu\nu\lambda}^{abc}(k_1, k_2, x'p', p_c), \quad (5)$$

the matrix elements in the polarized nucleon (bottom blob),

$$M_{abc}^{\mu\nu\lambda}(k_1, k_2) = g \int d^4\xi \int d^4\eta e^{ik_1\xi} e^{i(k_2-k_1)\eta} \langle pS_\perp | A_b^\nu(0) A_c^\lambda(\eta) A_a^\mu(\xi) | pS_\perp \rangle, \quad (6)$$

the unpolarized parton density (top blob) and the fragmentation function (second top blob) are convoluted. In (5) and (6), a, b, c are color indices, and $k_{1,2}$ are the momenta of the gluon lines before collinear expansion as assigned in Fig. 1. $x'p'$ is the momentum of the parton coming out of the unpolarized nucleon and $p_c \equiv P_h/z$ is the one for the parton fragmenting into the final hadron.

Figures 2-8 represent the leading order (LO) diagrams for $S_{\mu\nu\lambda}^{abc}(k_1, k_2, x'p', p_c)$. The real cross section occurs from a pole part of the propagator with a short bar in the diagrams, which gives rise to the soft-gluon-pole (SGP) contributions at $x_1 = x_2$. The diagrams have

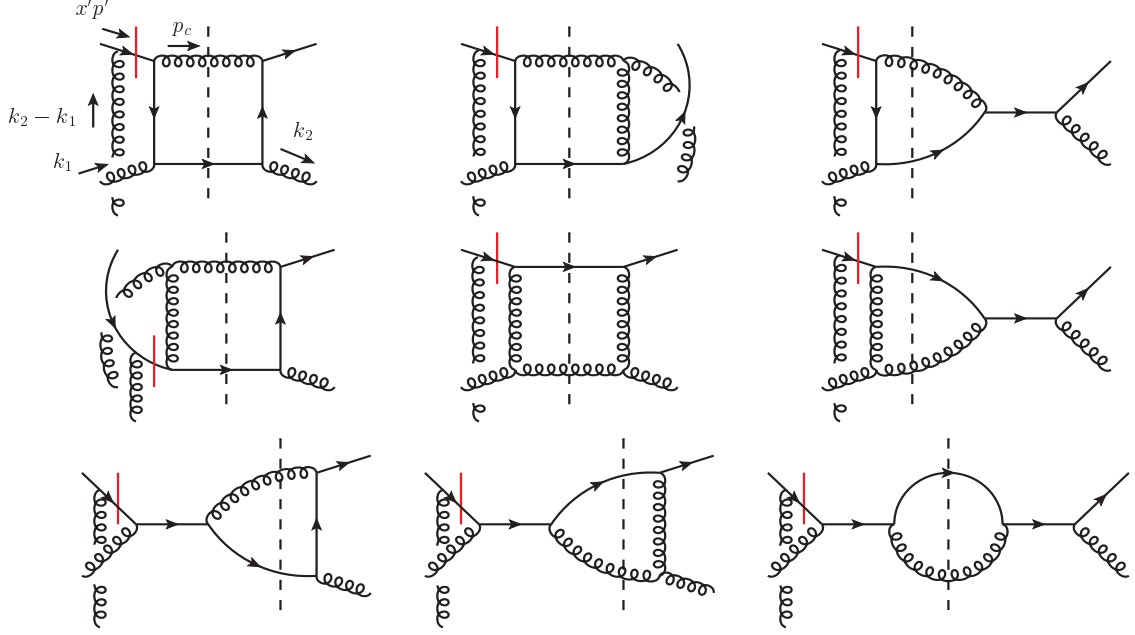


Figure 2: ISI diagrams in the gluon-fragmentation channel with the unpolarized quark distribution. Shift of the momentum p_c from the cut gluon-line to the cut quark-line produces diagrams in the quark-fragmentation channel with the unpolarized quark distribution, and the cross sections in these two channels are connected by $\hat{t} \leftrightarrow \hat{u}$.

the structure that an extra gluon line with the momentum $k_2 - k_1$ is attached to either initial- or final- parton line in the diagrams representing the twist-2 cross section, and the propagator next to the attachment gives a pole. Therefore the diagrams are classified as the initial-state-interaction (ISI) diagrams (Figs. 2, 5, 7) and the final state interaction (FSI) diagrams (Figs. 3, 4, 6, 8). We shall employ the convention that the QCD coupling constant g associated with the attachment of the extra gluon to $S_{\mu\nu\lambda}^{abc}$ is included in the matrix element (6) consistently with the definition of the three-gluon correlation functions in (1) and (2). The mirror diagrams of Figs. 2-8 also contribute, and other pole contributions cancel among each other by taking the sum of the whole diagrams.

Applying the collinear expansion to the pole contribution of $S_{\mu\nu\lambda}^{abc}(k_1, k_2, x'p', p_c)$, the LO twist-3 cross section induced by the three-gluon correlation function is obtained as

$$\begin{aligned}
 P_h^0 \frac{d\Delta\sigma}{d^3P_h} &= \frac{\alpha_s^2}{S} \sum_{i,j} \int \frac{dx'}{x'} f_i(x') \int \frac{dz}{z^2} D_j(z) \int \frac{dx_1}{x_1} \int \frac{dx_2}{x_2} \\
 &\quad \times \left[\frac{\partial S_{\mu\nu\lambda}^{abc}(k_1, k_2, x'p', p_c) p^\lambda}{\partial k_2^\sigma} \Big|_{k_i=x_i p} \right]_{\text{pole}} \omega^\mu_\alpha \omega^\nu_\beta \omega^\sigma_\gamma M_{F,abc}^{\alpha\beta\gamma}(x_1, x_2), \quad (7)
 \end{aligned}$$

where $\omega^\mu_\alpha = g^\mu_\alpha - p^\mu n_\alpha$, $f_i(x')$ and $D_i(z)$ are, respectively, unpolarized distribution and

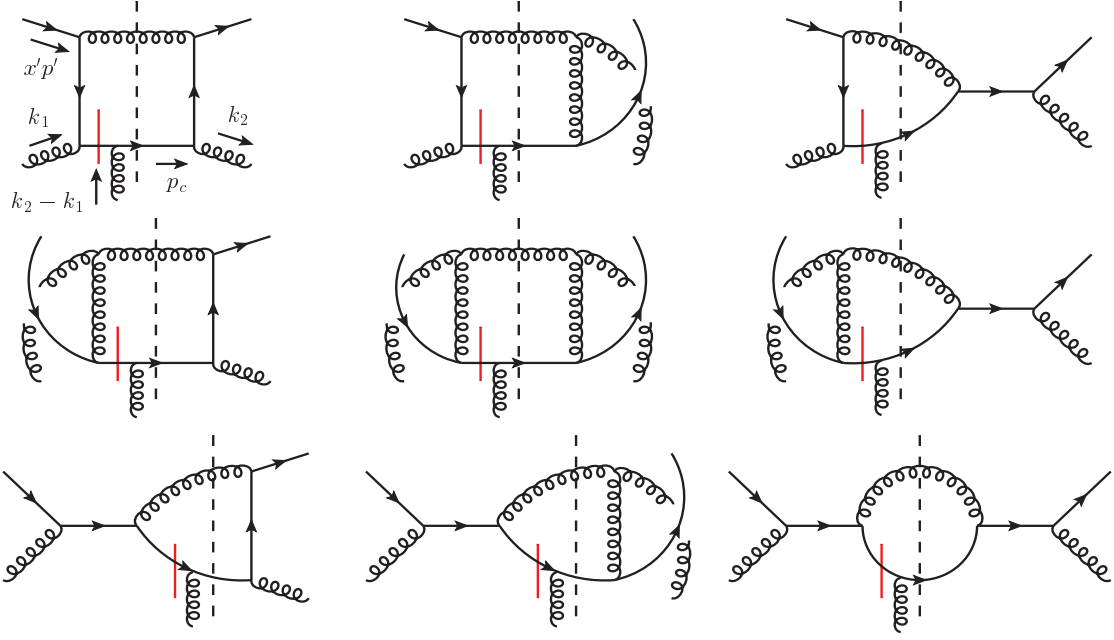


Figure 3: FSI diagrams in the quark-fragmentation channel with the unpolarized quark distribution.

fragmentation functions for the quark and anti-quark flavors and the gluon ($i = q, \bar{q}, g$), and $M_{F,abc}^{\alpha\beta\gamma}(x_1, x_2)$ is the lightcone correlation function of the field-strengths defined as

$$\begin{aligned}
M_{F,abc}^{\alpha\beta\gamma}(x_1, x_2) &= -g(i)^3 \int \frac{d\lambda}{2\pi} \int \frac{d\mu}{2\pi} e^{i\lambda x_1} e^{i\mu(x_2-x_1)} \langle pS_\perp | F_b^{\beta n}(0) F_c^{\gamma n}(\mu n) F_a^{\alpha n}(\lambda n) | pS_\perp \rangle \\
&= \frac{Nd_{bca}}{(N^2-4)(N^2-1)} O^{\alpha\beta\gamma}(x_1, x_2) - \frac{if_{bca}}{N(N^2-1)} N^{\alpha\beta\gamma}(x_1, x_2)
\end{aligned} \quad (8)$$

with $O^{\alpha\beta\gamma}(x_1, x_2)$ and $N^{\alpha\beta\gamma}(x_1, x_2)$ defined in (1) and (2), respectively. The symbol $[\dots]^{\text{pole}}$ indicates the pole contribution is to be taken from the barred propagator in the hard part. In (7), the factor g^4 is shifted to a prefactor from the hard part $S_{\mu\nu\lambda}^{abc}$. We remind that even though the analysis of Figs. 2-8 starts with the gauge-noninvariant correlation function (6) and the corresponding hard part $S_{\mu\nu\lambda}^{abc}(k_1, k_2, x'p', p_c)$, gauge-noninvariant contributions appearing in the collinear expansion either vanish or cancel and the total surviving twist-3 contribution to the single-spin-dependent cross section can be expressed as in (7), using the gauge-invariant correlation functions (1) and (2).

By calculating $\left[\partial S_{\mu\nu\lambda}^{abc}(k_1, k_2, x'p', p_c) p^\lambda / \partial k_2^\sigma \Big|_{k_i=x_i p} \right]^{\text{pole}}$ from Figs. 2-8 contracted with the coefficient tensors in the decomposition of (1) and (2), one obtains the twist-3 single-

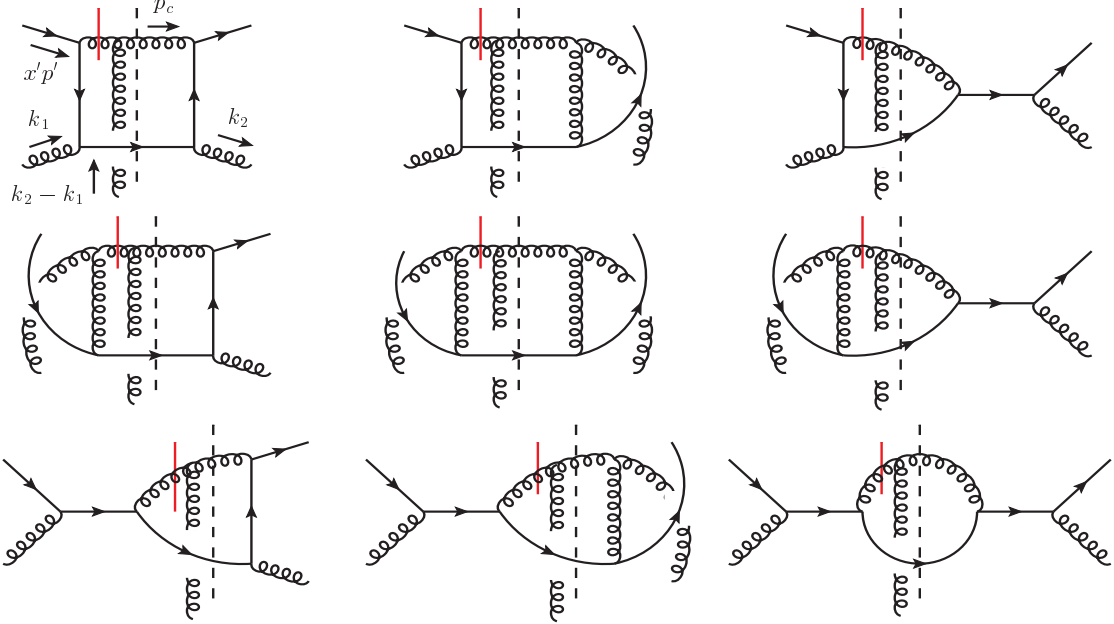


Figure 4: FSI diagrams in the gluon-fragmentation channel with the unpolarized quark distribution.

spin-dependent cross section as

$$\begin{aligned}
 E_{P_h} \frac{d^3 \Delta \sigma}{d^3 P_h} &= \frac{2\pi M_N \alpha_s^2}{S} \epsilon^{P_h p_n S \perp} \sum_{i,j} \int \frac{dx}{x} \int \frac{dx'}{x'} f_i(x') \int \frac{dz}{z^2} D_j(z) \delta(\hat{s} + \hat{t} + \hat{u}) \frac{1}{z\hat{u}} \\
 &\times \left[\zeta_{ij} \left(\frac{d}{dx} O(x) - \frac{2O(x)}{x} \right) \hat{\sigma}_{gi \rightarrow j}^{(O)} + \left(\frac{d}{dx} N(x) - \frac{2N(x)}{x} \right) \hat{\sigma}_{gi \rightarrow j}^{(N)} \right], \quad (9)
 \end{aligned}$$

where the functions $O(x)$ and $N(x)$ are defined as

$$O(x) \equiv O(x, x) + O(x, 0), \quad N(x) \equiv N(x, x) - N(x, 0), \quad (10)$$

and the factor ζ_{ij} is defined so that $\zeta_{ij} = -1$ when i or j is an anti-quark flavor and $\zeta_{ij} = 1$ for other cases. The partonic hard cross sections $\hat{\sigma}_{gi \rightarrow j}^{(O,N)}$ are the functions of the partonic Mandelstam variables defined as¹

$$\hat{s} = (xp + x'p')^2, \quad \hat{t} = (xp - p_c)^2, \quad \hat{u} = (x'p' - p_c)^2, \quad (11)$$

and can be written as the sum of the contributions from the ISI and FSI diagrams:

$$\hat{\sigma}_{gi \rightarrow j}^{(O,N)} = \hat{\sigma}_{gi \rightarrow j}^{(O,N)I} - \frac{\hat{S}}{\hat{t}} \hat{\sigma}_{gi \rightarrow j}^{(O,N)F}. \quad (12)$$

¹The cross section (9) is a function of the Mandelstam variables $S = (p + p')^2$, $T = (p - P_h)^2$ and $U = (p' - P_h)^2$.

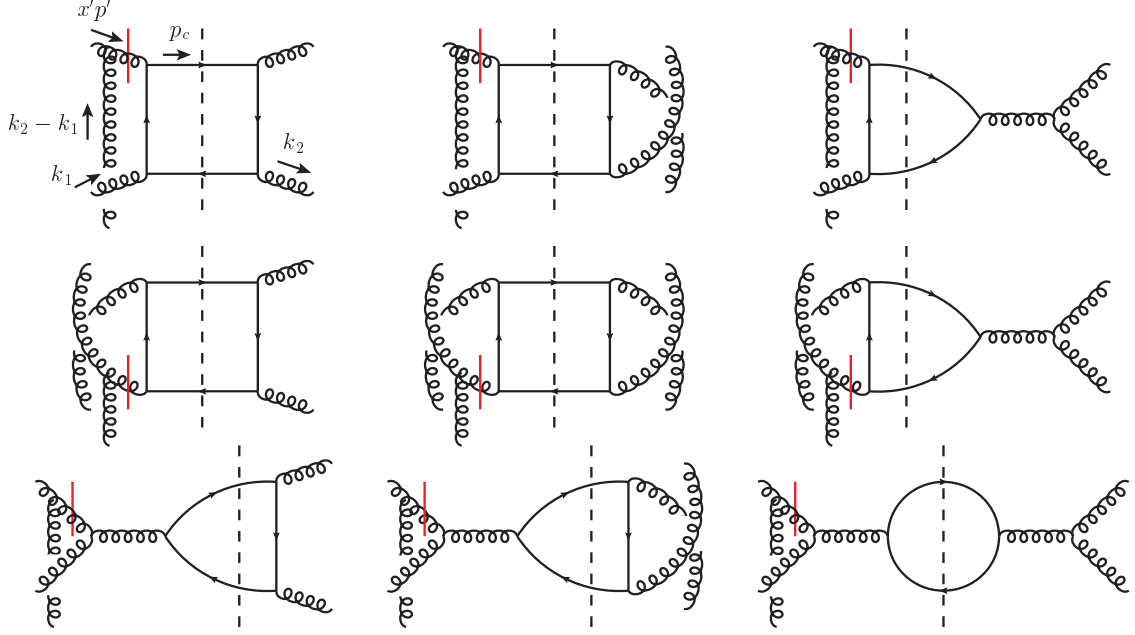


Figure 5: ISI diagrams in the quark-fragmentation channel with the unpolarized gluon distribution.

They are given as follows:

(i) Unpolarized quark distribution channels:

(a) Quark fragmentation channel (Figs. 2, 3):

$$\hat{\sigma}_{gq \rightarrow q}^{(O)I} = -\hat{\sigma}_{gq \rightarrow q}^{(N)I} = \frac{\hat{t}(\hat{s}^2 + \hat{t}^2)}{\hat{s}\hat{u}^2} - \frac{1}{N^2} \left(\frac{\hat{s}}{\hat{t}} + \frac{\hat{t}}{\hat{s}} \right), \quad (13)$$

$$\hat{\sigma}_{gq \rightarrow q}^{(O)F} = \hat{\sigma}_{gq \rightarrow q}^{(N)F} = -\frac{\hat{s}(\hat{s}^2 + \hat{t}^2)}{\hat{t}\hat{u}^2} + \frac{1}{N^2} \left(\frac{\hat{s}}{\hat{t}} + \frac{\hat{t}}{\hat{s}} \right). \quad (14)$$

(a) Gluon fragmentation channel (Figs. 2, 4) :

$$\hat{\sigma}_{gq \rightarrow g}^{(O)I} = -\hat{\sigma}_{gq \rightarrow g}^{(N)I} = \frac{\hat{u}(\hat{s}^2 + \hat{u}^2)}{\hat{s}\hat{t}^2} - \frac{1}{N^2} \left(\frac{\hat{s}}{\hat{u}} + \frac{\hat{u}}{\hat{s}} \right), \quad (15)$$

$$\hat{\sigma}_{gq \rightarrow g}^{(O)F} = \frac{(\hat{s} - \hat{u})(\hat{s}^2 + \hat{u}^2)}{\hat{s}\hat{t}\hat{u}}, \quad (16)$$

$$\hat{\sigma}_{gq \rightarrow g}^{(N)F} = \frac{(\hat{s}^2 + \hat{u}^2)^2}{\hat{s}\hat{t}^2\hat{u}}, \quad (17)$$

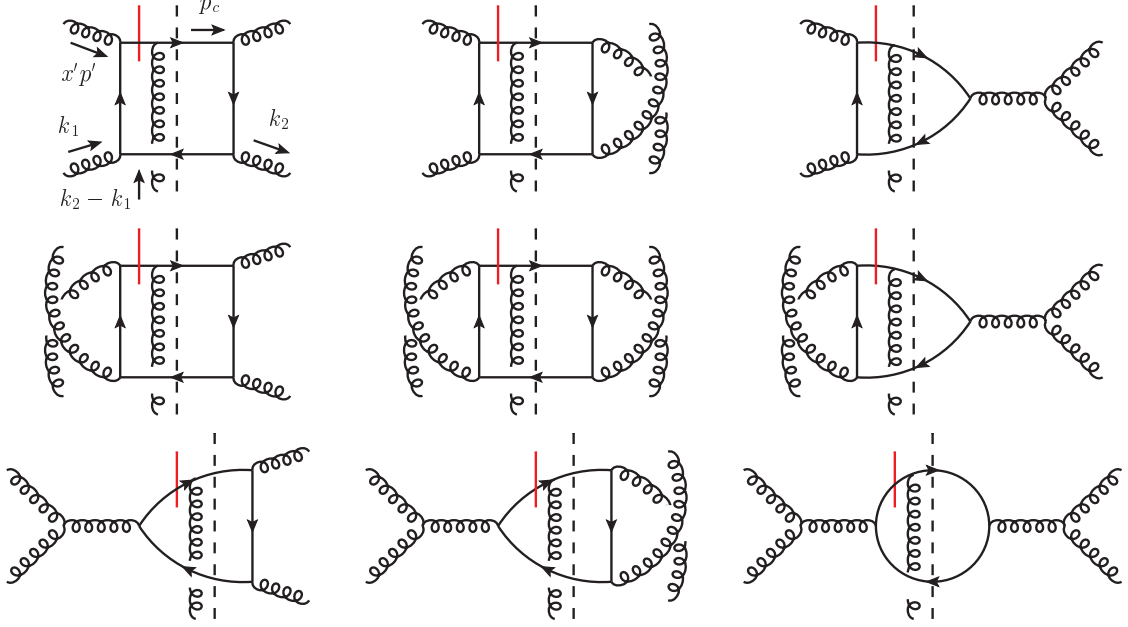


Figure 6: FSI diagrams in the quark-fragmentation channel with the unpolarized gluon distribution.

(ii) Unpolarized gluon distribution channels:

(b) Quark fragmentation channel (Figs. 5, 6):

$$\hat{\sigma}_{gg \rightarrow q}^{(O)I} = \frac{1}{C_F} \frac{(\hat{u} - \hat{t})(\hat{t}^2 + \hat{u}^2)}{2\hat{s}\hat{t}\hat{u}}, \quad (18)$$

$$\hat{\sigma}_{gg \rightarrow q}^{(N)I} = \frac{1}{C_F} \frac{(\hat{t}^2 + \hat{u}^2)^2}{2\hat{s}^2\hat{t}\hat{u}}, \quad (19)$$

$$\hat{\sigma}_{gg \rightarrow q}^{(O)F} = \hat{\sigma}_{gg \rightarrow q}^{(N)F} = \left(-\frac{1}{C_F} \frac{\hat{u}}{2\hat{s}^2\hat{t}} + \frac{1}{N^2 C_F} \frac{1}{2\hat{t}\hat{u}} \right) (\hat{t}^2 + \hat{u}^2). \quad (20)$$

(b) Gluon fragmentation channel (Figs. 7, 8):

$$\hat{\sigma}_{gg \rightarrow g}^{(O)I,F} = 0, \quad (21)$$

$$\hat{\sigma}_{gg \rightarrow g}^{(N)I} = \frac{N}{C_F} \frac{2(\hat{t}^2 + \hat{u}^2)(\hat{t}^2 + \hat{t}\hat{u} + \hat{u}^2)^2}{\hat{s}^2\hat{t}^2\hat{u}^2}, \quad (22)$$

$$\hat{\sigma}_{gg \rightarrow g}^{(N)F} = -\frac{N}{C_F} \frac{2(\hat{t}^2 + 2\hat{t}\hat{u} + 2\hat{u}^2)(\hat{t}^2 + \hat{t}\hat{u} + \hat{u}^2)^2}{\hat{s}^2\hat{t}^2\hat{u}^2}. \quad (23)$$

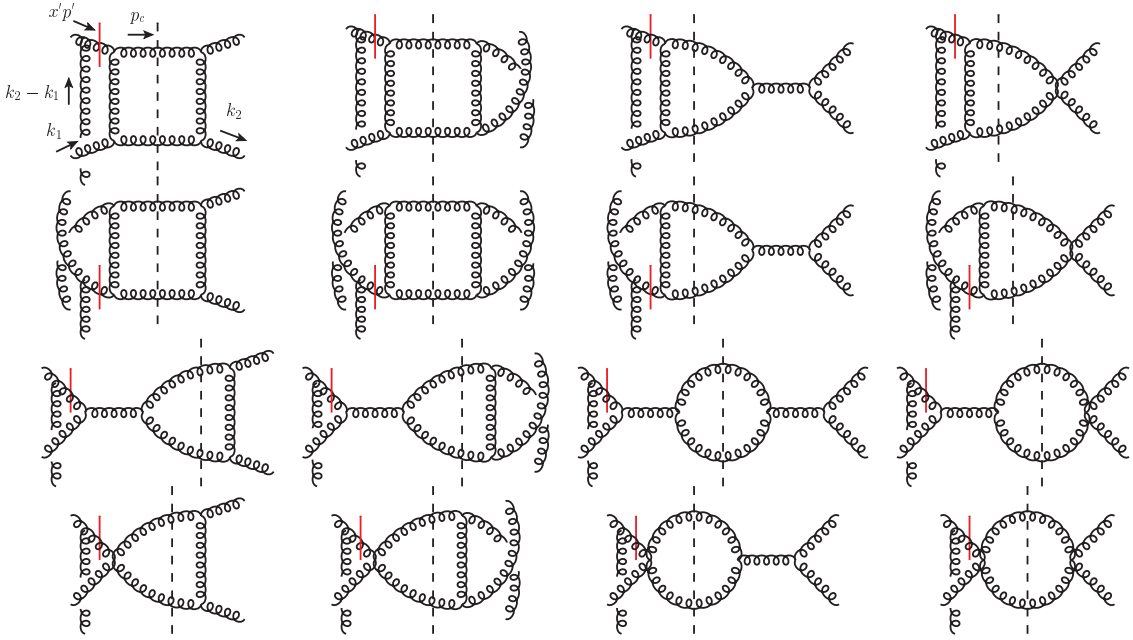


Figure 7: ISI diagrams in the gluon-fragmentation channel with the unpolarized gluon distribution.

A remarkable feature of (9) is that the partonic hard cross sections for $O(x, x)$ and $O(x, 0)$ are identical, and likewise for $N(x, x)$ and $-N(x, 0)$. Therefore they contribute to the cross section through the combinations $O(x)$ and $N(x)$ in (10). The same feature was also observed for the twist-3 cross section for the prompt-photon production $p^\uparrow p \rightarrow \gamma X$. Note that (18), (19) and (20) are obtained from the result for $p^\uparrow p \rightarrow DX$ in [20] by taking the massless limit of the charm-quark mass, $m_c \rightarrow 0$. For the processes in which all partons participating in the scattering are massless, three-gluon correlations contribute in the combination of $O(x)$ and $N(x)$. This is in contrast to the case for SIDIS and Drell-Yan processes, where the virtual photon with large Q^2 enters the scattering. The result $\hat{\sigma}_{gg \rightarrow g}^{(O)I,F} = 0$ in (21) is due the vanishing color factors.

4 Numerical calculation of the asymmetry at the RHIC energy

To illustrate the effect of the three-gluon correlation functions to A_N for the light-hadron production, we will present a model calculation of A_N at the RHIC energy. To this end, we employ the same models which were used for the study of A_N in $p^\uparrow p \rightarrow DX$ and $p^\uparrow p \rightarrow \gamma X$ [20, 21]. They are parametrized by using the twist-2 unpolarized gluon density $G(x)$ as

$$\text{Model 1 : } O(x) = N(x) = 0.004 x G(x), \quad (24)$$

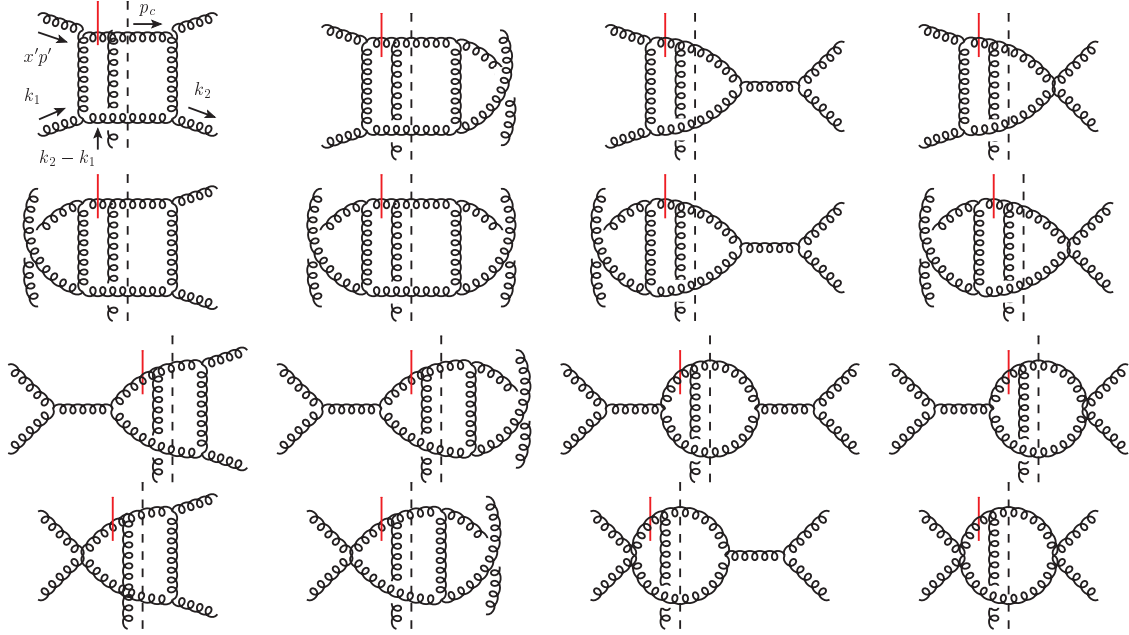


Figure 8: FSI diagrams in the gluon-fragmentation channel with the unpolarized gluon distribution.

$$\text{Model 2 : } O(x) = N(x) = 0.001\sqrt{x}G(x), \quad (25)$$

and the scale dependence of the three-gluon correlation is also assumed to follow these relations.² The coefficients 0.004 and 0.001 were determined so that the calculated A_N^D does not exceed the RHIC preliminary data for A_N^D [33]. The above model ansatz was motivated to see the effect of the three-gluon correlations in comparison with the gluon density and to see the sensitivity of A_N to the small- x behavior of the functions. We use the unpolarized parton density in [34] and the fragmentation function for the pion in [35]. For the calculation, we set the scale of all the distribution and fragmentation functions at the transverse momentum of the final hadron P_T .

Figure 9 shows the x_F -dependence of the three-gluon contribution to A_N for the $\pi^{\pm,0}$ and jet productions in the pp-collision at the RHIC energy $\sqrt{S} = 200$ GeV and $P_T = 2$ GeV. We plotted the contribution from $O(x)$ and $N(x)$ separately to see each effect on A_N . At $x_F > 0$, $N(x)$ gives rise to the large asymmetry and the effect of $O(x)$ is negligible for both models. The origin of the large asymmetry from $N(x)$ is the partonic cross section (23): At large $x_F > 0$, where $-T \ll S \sim -U$, large- x and small- x' region is probed, and thus the unpolarized gluon density brings main contribution. While the partonic cross sections in the quark fragmentation channel (18)-(20) are tiny, those in the gluon fragmentation

²The evolution equation for the three-gluon correlation functions $O(x_1, x_2)$ and $N(x_1, x_2)$ has been derived in [17]. For this first rough estimate of A_N , however, we use a simplified model as above.

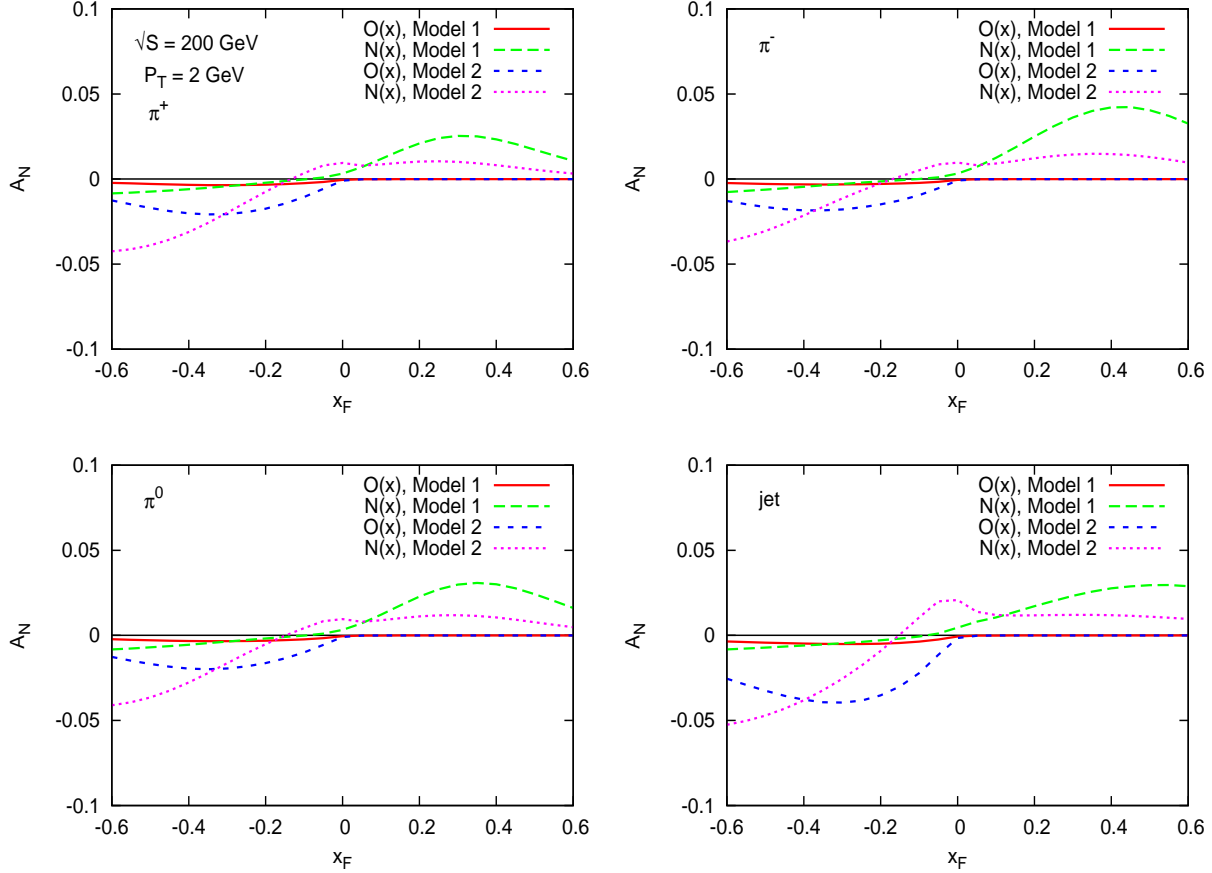


Figure 9: x_F -dependence of the three-gluon contribution to A_N for $p^\uparrow p \rightarrow \{\pi^{\pm,0}, \text{jet}\} X$ at $\sqrt{S} = 200$ GeV and $P_T = 2$ GeV. The contribution from $O(x)$ and $N(x)$ are plotted separately for models 1 and 2.

channel (22) and (23) for $N(x)$ are large, in particular, the latter contribution is enhanced by the kinematic factor \hat{s}/\hat{t} in (12) for the FSI.

At $x_F < 0$, in particular, $x_F \rightarrow -1$ where $-U \ll S \sim -T$, the region of small- x and large- x' is relevant. Thus the model 1 gives rise to only small asymmetry for both $O(x)$ and $N(x)$ due to their mild behavior at small- x . On the other hand, the model 2 gives the large asymmetry for the two functions. This is due to the large partonic cross section (13) and (14) in the unpolarized quark distribution channel with the quark fragmentation, and a steeply rising behavior in the three-gluon correlations at small- x , which is even more enhanced by the derivative. For $O(x)$, there is a partial cancelation between the ISI and FSI due to the relative signs between (13) and (14), while for $N(x)$ these cross sections contribute constructively. This leads to different behavior of the asymmetry between $N(x)$ and $O(x)$.

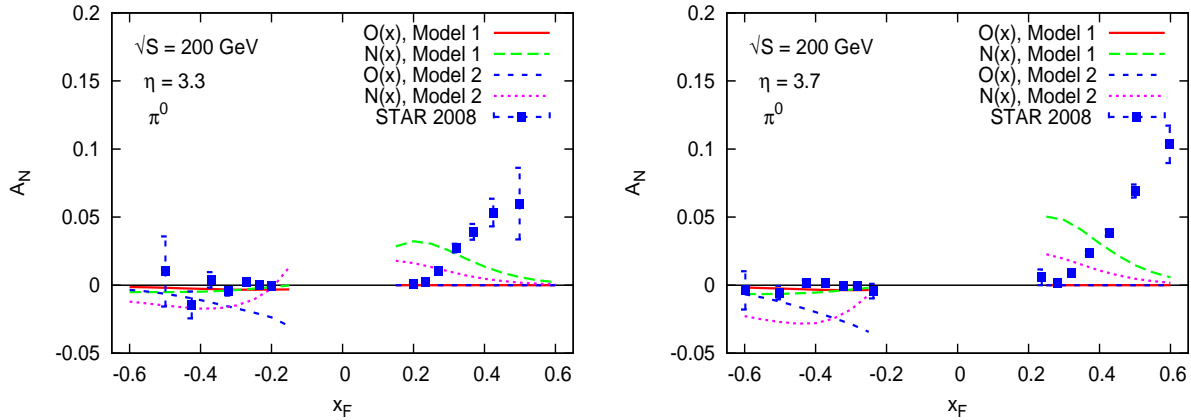


Figure 10: x_F -dependence of the three-gluon contribution to A_N for $p^\uparrow p \rightarrow \pi^0 X$ at $\sqrt{S} = 200$ GeV and $\eta = 3.3$ and 3.7 in comparison to the RHIC-STAR data [3]. The contribution from $O(x)$ and $N(x)$ are plotted separately for models 1 and 2.

Figure 10 shows the three-gluon contribution to $A_N^{\pi^0}$ in comparison to the RHIC-STAR data [3] at $\sqrt{S} = 200$ GeV and the pseudorapidity $\eta = 3.3$ and 3.7 . One sees that the contribution from $N(x)$ is much larger than the data at small $x_F > 0$ for the two models, and therefore it is unlikely that the magnitude of $N(x)$ is as large as these models in the large- x region. At $x_F < 0$, the contribution of the model 1 is zero and is consistent with data for both $N(x)$ and $O(x)$, while the model 2 for the two functions is far from the data points. This means the three-gluon correlations should behave more mildly than the model 2 in the small- x region. We note, however, that the observed asymmetry results from the combination of the quark-gluon correlation function, twist-3 fragmentation function and the three-gluon correlation function, and thus we need a complete analysis including all these effects to draw a definite conclusion.

Figure 11 shows the calculated $A_N^{\pi^0}$ in the midrapidity region ($|\eta| < 0.35$) at $\sqrt{S} = 200$ GeV in comparison with the RHIC-PHENIX data [8]. Both models give tiny asymmetry due to the small partonic cross sections, so the form of the three-gluon correlation functions is not much constrained by the data in this region.

5 Summary

In this paper we have studied the three-gluon contribution to SSA for the light hadron production in the pp collision, $p^\uparrow p \rightarrow hX$. We have derived the corresponding LO twist-3 cross section. Together with the result for the contribution from the quark-gluon correlation and the twist-3 fragmentation functions, this has completed the twist-3 cross section for this process. We have also presented a numerical calculation of the asymmetry at the RHIC

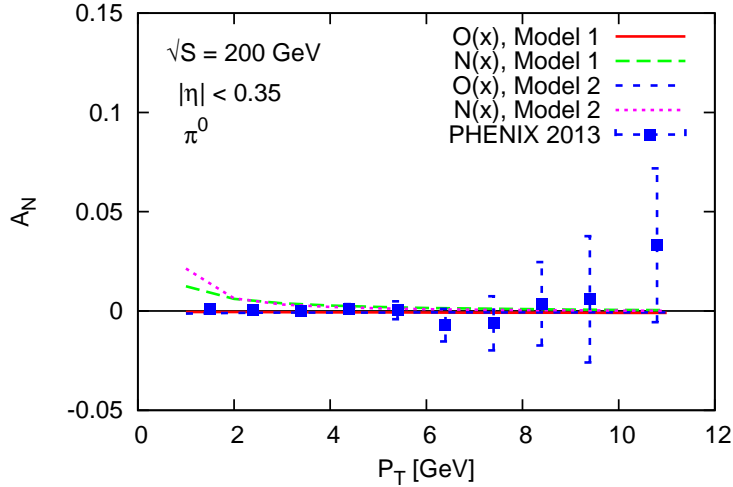


Figure 11: P_T -dependence of the three-gluon contribution to A_N for $p^\uparrow p \rightarrow \pi^0 X$ at $\sqrt{S} = 200$ GeV and $|\eta| < 0.35$ in comparison to the RHIC-PHENIX data [8]. The contribution from $O(x)$ and $N(x)$ are plotted separately for models 1 and 2.

energy based on our previous models and have shown that this process could bring a useful constraint on the upper bound of the three-gluon correlation functions.

Acknowledgments

The work of K.K. is supported by the Grand-in-Aid for Scientific Research (No.24.6959) from the Japan Society of Promotion of Science. The work of Y.K. is supported in part by the Grant-in-Aid for Scientific Research (No.23540292) from the Japan Society of Promotion of Science. The work of S.Y. is supported by JSPS Strategic Young Researcher Overseas Visits Program for Accelerating Brain Circulation (No.R2411) .

References

- [1] J. Adams, et al., STAR Collaboration, Phys. Rev. Lett. 92 (2004) 171801.
- [2] S. S. Adler, et al., PHENIX Collaboration, Phys. Rev. Lett. 95 (2005) 202001.
- [3] B. I. Abelev, et al., STAR Collaboration, Phys. Rev. Lett. 101 (2008) 222001.
- [4] I. Arsene, et al., BRAHMS Collaboration, Phys. Rev. Lett. 101 (2008) 042001.
- [5] L. Adamczyk, et al., STAR Collaboration, Phys. Rev. D 86 (2012) 051101.

- [6] L. Adamczyk, et al., STAR Collaboration, Phys. Rev. D 86 (2012) 032006.
- [7] L. Adamczyk *et al.* [STAR Collaboration], arXiv:1309.1800 [nucl-ex].
- [8] A. Adare, et al., PHENIX Collaboration, arXiv:1312.1995 [hep-ex].
- [9] J. Qiu, G. Sterman, Nucl. Phys. B 378 (1992) 52.
- [10] J. Qiu, G. Sterman, Phys. Rev. D 59 (1998) 014004.
- [11] H. Eguchi, Y. Koike, K. Tanaka, Nucl. Phys. B 752 (2006) 1.
- [12] H. Eguchi, Y. Koike, and K. Tanaka, Nucl. Phys. B **763**, 198 (2007).
- [13] C. Kouvaris, J.-W. Qiu, W. Vogelsang, F. Yuan, Phys. Rev. D 74 (2006) 114013.
- [14] Y. Koike, K. Tanaka, Phys. Rev. D 76 (2007) 011502.
- [15] Y. Koike, T. Tomita, Phys. Lett. B 675 (2009) 181.
- [16] A. V. Belitsky, X. D. Ji, W. Lu, J. Osborne, Phys. Rev. **D63**, 094012 (2001).
- [17] V.M. Braun, A.N. Manashov, B. Pirnay, Phys. Rev. **D80**, 114002 (2009).
- [18] H. Beppu, Y. Koike, K. Tanaka, and S. Yoshida, Phys. Rev. D **82**, 054005 (2010).
- [19] Y. Koike, K. Tanaka, and S. Yoshida, Phys. Rev. D **83**, 114014 (2011).
- [20] Y. Koike, S. Yoshida, Phys. Rev. D 84 (2011) 014026.
- [21] Y. Koike, S. Yoshida, Phys. Rev. D 85 (2012) 034030.
- [22] X. Ji, Phys. Rev. D **49**, 114 (1994).
- [23] F. Yuan, J. Zhou, Phys. Rev. Lett. 103 (2009) 052001.
- [24] Z.-B. Kang, F. Yuan, J. Zhou, Phys. Lett. B 691 (2010) 243.
- [25] A. Metz and D. Pitonyak, Phys. Lett. B **723**, 365 (2013).
- [26] Y. Kanazawa, Y. Koike, Phys. Lett. B 478 (2000) 121.
- [27] Y. Kanazawa, Y. Koike, Phys. Lett. B 490 (2000) 99.
- [28] K. Kanazawa, Y. Koike, Phys. Rev. D 82 (2010) 034009.
- [29] K. Kanazawa, Y. Koike, Phys. Rev. D 83 (2011) 114024.
- [30] K. Kanazawa and Y. Koike, Phys. Lett. B **720** (2013) 161.
- [31] Z. -B. Kang, J. -W. Qiu, W. Vogelsang and F. Yuan, Phys. Rev. D **83**, 094001 (2011).

- [32] H. Beppu, Y. Koike, K. Tanaka, S. Yoshida, Phys. Rev. D 85 (2012) 114026.
- [33] H. Liu [PHENIX Collaboration], AIP Conf. Proc. **1149** (2009) 439.
- [34] M. Gluck, P. Jimenez-Delgado, and E. Reya, Eur. Phys. J. **C53** 355 (2008).
- [35] D. de Florian, R. Sassot, and M. Stratmann, Phys. Rev. D **75**, 114010 (2007).